Journal of Biophysical Chemistry, 2015, 6, 1-13
Published Online February 2015 in SciRes. http://www.scirp.org/journal/jbpc
http://dx.doi.org/10.4236/jbpc.2015.61001

Chlorambucil Encapsulation into PLGA Nanoparticles and Cytotoxic Effects in Breast Cancer Cell

Diego J. S. Dias[1,2], Graziella A. Joanitti[3], Ricardo B. Azevedo[2], Luciano P. Silva[4], Claure N. Lunardi[1,3], Anderson J. Gomes[1,3*]

[1]School of Health Sciences, University of Brasilia, Brasilia, Brazil
[2]Institute of Biological Sciences, University of Brasilia, Brasilia, Brazil
[3]Laboratory of Nanobiotechnology, Faculty of Ceilandia, University of Brasilia, Brasilia, Brazil
[4]Laboratory of Mass Spectrometry, EMBRAPA, Genetic Resources and Biotechnology, Brasilia, Brazil
Email: *ajgomes@unb.br, clunardi@unb.br

Received 30 October 2014; revised 28 November 2014; accepted 29 December 2014

Abstract

The present work aimed to develop and evaluate a colloidal system composed of poly (DL-lactide-co-glycolide) (PLGA) nanoparticles (NPs) associated with chlorambucil (CHB) and its effects on cancer cells. The nanoparticles showed %EE (>92%), a mean particle size in the range of 240 to 334 nm and zeta potential of −16.7 to −26.0 mV. *In vitro* release profile showed a biphasic pattern, with an initial burst for all formulations. The scanning electron microscopy of CHB-nanoparticles showed regular spherical shapes, smooth surface without aggregations. Differential scanning calorimetry thermograms, UV-vis absorption, fluorescence emission and Fourier transform infrared spectroscopy were performed showing the entrapment of the antitumoral in drug delivery system. CHB encapsulated in PLGA nanoparticles decrease the survival rates of the breast cancer cells: 68.9% reduction of cell viability on MCF-7 cell line and 59.7% on NIH3T3. Our results indicated that polymeric nanoparticles produced by classical methods are efficient drug delivery systems for CHB.

Keywords

Chlorambucil, PLGA, Nanoparticles, Cancer, MCF-7

*Corresponding author.

How to cite this paper: Dias, D.J.S., *et al.* (2015) Chlorambucil Encapsulation into PLGA Nanoparticles and Cytotoxic Effects in Breast Cancer Cell. *Journal of Biophysical Chemistry*, **6**, 1-13. http://dx.doi.org/10.4236/jbpc.2015.61001

1. Introduction

Breast cancer is the leading diagnosed cancer and the most common cause of cancer-related death in women worldwide [1]-[3]. Several chemotherapeutic drugs are used in the treatment of breast cancer to reduce or suppress the growth of cancerous cells [1] [4]-[7]. Alkylating agents, such as chlorambucil (4-[p-[bis [2-chloroethyl] amino] phenyl]-butanoic acid (CHB), are extensively used in the treatment of neoplastic diseases, such as chronic lymphocytic leukemia, lymphomas, advanced ovarian and breast cancer [1] [8]. However, chlorambucil use is limited by its toxic side effects, including myelotoxicity and neurotoxicity [9] [10]. These adverse profiles, limit the use of optimal doses of chemotherapeutic drug CHB. Consequently, protocols with sub-optimal doses are frequently used, minimizing toxicity and patient suffering but often resulting in inefficient treatment and unsatisfactory prognosis [11]. Ganta and coworkers [12] investigate the pharmacokinetics, tissue distribution, and anticancer activity of CHB and chlorambucil-loaded parenteral emulsion (CHL-PE) in C57 BL/6 mice. Yordanov and coworkers [13] show the preparation and physicochemical characterization of chlorambucil-loaded poly(butylcyanoacrylate) nanoparticles. Descoteaux and coworkers [14] synthesized L-tyro-sine-Chlorambucil analogs and evaluate their effects as anticancer drugs on MCF-7 cell line. These analogs showed significant anticancer activities compare to Chlorambucil. Also Omoomi [15] show the production of a new anticancer conjugate of Chlorambucil-Methionine which is highly effective, and has selective targeting features, as well as the ability to prevent the growth of the breast cancer MCF-7 cell line. Millard and coworkers [16] synthetized Mito-Chlor, a triphenylphosphonium derivative of the CHB which selectively targeting nitrogen mustards to cancer cell mitochondria based on mitochondrial membrane potential.

A promising approach to prevent harmful side effects and to increase drug bioavailability and the fraction of the drug accumulated in the required zone, is the entrapment of drug in appropriate drug delivery systems [17] [18]. In recent years, much research has been focused on the application of biocompatible and biodegradable polymers to drug delivery systems [19]-[22]. Among those polymers, a significant one has been the poly (DL-lactide-co-glycolide) (PLGA) [23]-[26]. Encapsulation of drugs in PLGA matrices from which they are released at a relatively slow rate over a prolonged time allows less frequent administrations, thereby increasing patient compliance and reducing discomfort, protection of the therapeutic compound within the body, and avoidance of peak-related side effects by maintaining more-constant blood levels of the drug [27]. The aim of present study is the investigation of the manufacturing parameters to obtain the best formulations of PLGA particles leading to reduced size and higher %EE to evaluate the cytotoxicity activity in both MCF-7 breast cancer cells and fibroblast NIH3T3 cells.

2. Experimental

2.1. Materials

Chlorambucil, poly(lactic-co-glycolic) acid (PLGA 50:50, Mw 17 kDa) and 3-(4,5-dimethylthiazol-2-yl)-2,5-diphenyl tetrazolium bromide (MTT) were obtained from Sigma Chemical (St. Louis, MO, USA); poly(vinyl alcohol) (PVA) (13 - 23 kDa, 87% - 89% hydrolyzed) was supplied by Aldrich (Milwaukee, WI, USA). Dichloromethane and dimethylsulfoxide (DMSO) of analytical grade were supplied by Merck (Darmstadt, Germany). Dulbecco's modified Eagle's medium (DMEM), Fetal Bovine Serum (FBS), penicillin and streptomycin (Gibco-BRL; Grand Island, NY). All other chemicals were of analytical grade and used without further purification.

2.2. Preparation of Nanoparticles by Solvent Evaporation Technique (CHB-NP I)

Nanoparticles (CHB-NP I) were produced by solvent evaporation method [28]-[30]. Briefly, 0.1 g of PLGA 50:50 and 10, 20 and 30 mg of CHB were dissolved in 10 mL of dichloromethane CH_2Cl_2. The dispersed phase was dropped into 20 mL of an aqueous phase containing 2.0% (w/v) of PVA, under ice cooling with stirring at 17,000 rpm for 3 min. Afterwards, solvent evaporation was carried out by gentle magnetic stirring at room temperature. Nanoparticles were recovered by centrifugation at 25,000 g for 10 min at 4˚C, washed with distilled water at 10˚C, and stored under refrigeration. Blank nanoparticles were used as a control.

2.3. Preparation of Nanoparticles by Double Emulsion Technique (CHB-NP II)

The preparation CHB-NP II was achieved by adjusting the double emulsion technique ($W_1/O/W_2$, water-in-oil-

in-water), previously applied to the preparation of other PLGA nanoparticles [31]-[34]. Briefly, chorambucil (10, 20, 30 mg) was solubilized in a mixture of methanol/water (1:1) and emulsified in methylene chloride (5.0 mL) containing PLGA (500 mg) using a highspeed homogenizer (Ultra-TurraxT25, IKA) for 60 s, at 17,000 rpm. The primary W/O emulsion was immediately transferred to 20 mL of a 2.0% (w/v) aqueous solution of PVA and homogenized under ice cooling, with stirring at 17,000 rpm for 2 min, using the high speed homogenizer. Afterwards, solvent evaporation was carried out by gentle magnetic stirring at room temperature, usually for 3 - 5 h. Nanoparticles were recovered by centrifugation for 10 min, at 25,000 g and 4˚C and washed (three times) with distilled water. After centrifugation, the NPs were stored at −4˚C. The encapsulation process was carried out under aseptic conditions. Nanoparticles without the drug were also prepared by the same procedure in order to evaluate the possible damage promoted by the particles itself.

The Encapsulation Efficiencies (%EEs) of both CHB-NP I and CHB-NP II were analyzed in relation to its %EE, for both formulations the volume equivalent to 5.0 mg of particles were weighed and dissolved in 5.0 mL methanol. For this process, the free drug are measured in organic medium methanol and the absorbance of this solution was taken and compared with a calibration curve and calculated in the same way using the Equation (1).

$$\%EE = \left(\text{Drug Loading}/\text{Theoretical Drug Loading}\right)\times 100\% \quad (1)$$

2.4. Nanoparticles Morphology: SM Analysis

Scanning Electron Microscopy (SM) was used to evaluate the shape and size of both CHB-NP I and CHB-NP II. Samples containing nanoparticles were placed on aluminum stubs coated with 50 nm gold coating under an argon atmosphere. CHB-NP I and II were examined and imaged by a Jeol 840 A (Tokyo, Japan) Scanning Electron Microscope operating at 20 kV in the traditional mode (SEI detector). Particle size was measured by using the software ImageJ® NIH.

2.5. Particle Size and Zeta Potential

Hydrodynamic diameter was determined by photon correlation spectroscopy (PCS) using the quasi-elastic light scattering technique, in a Zetasizer Nano ZS equipment (Malvern Instruments, Worcestershire, UK) equipped with a 10 mW He-Ne 633 nm laser beam, at 25˚C and at a scattering angle of 173˚. For the particle size analysis, a dilute suspension (1.0 mg/mL) of CHB-NP I and CHB-NP II were prepared in double distilled water and sonicated in an ice bath for 30 s. The zeta potential of the CHB-NP I and CHB-NP II in PBS buffer, (0.1 mmol, pH 7.4) was determined by using ZetaPlus™ in the zeta potential analysis mode.

2.6. Ultraviolet-Visible (UV-vis) and Fluorescence Spectroscopy

The UV-vis measurements were performed on Hitachi U-3900H UV-vis Spectrophotometer in the wavelength interval of 200 - 800 nm at 37˚C. Fluorescence spectra were recorded on a spectrofluorimeter (Hitachi F-7000) at 37˚C. Each spectrum was an average of three (from 280 to 550 nm) with a resolution of 1.0 nm. The chosen wavelength for excitation was 270 nm for CHB. Slits of 2.0 nm were used for excitation and emission.

2.7. Fourier Transform Infrared (FTIR) Spectroscopy

The chemical structure of the nanoparticles (unloaded and loaded with CHB-NP I and CHB-NP II) was analyzed by FTIR (IR Prestige-21 FTIR-8400S, Shimadzu, Japan) in transmission mode. For that, dried nanoparticles (1.0 mg) were mixed with KBr (40.0 mg) and then formed into a disc in a manual press. Transmission spectra were recorded using at least 32 scans with 4.0 cm^{-1} resolution, in the spectral range 4000 - 400 cm^{-1}.

2.8. Differential Scanning Calorimetry (DSC)

Thermal characterizations of CHB-NP I and CHB-NP II were performed with a Shimadzu DSC-60A. The equipment was calibrated with indium. The sample (approximately 3.0 mg) was heated twice from 35˚C to 600˚C at 5˚C/min in a nitrogen atmosphere (flow rate 20 mL/min). The melting temperature (T_m) was determined from the endothermic peak of the DSC curve recorded in the first heating scan. The glass transition temperature (T_g) was determined from the DSC curve recorded in the second heating scan.

2.9. Release Profile

The *in vitro* release analyses of the CHB-NP I and CHB-NP II were carried out in triplicate. Particles were added to 20 mL PBS buffer (10 mM; pH 7.4) in a conical flask shaken at 37˚C in a water bath at 65 rpm. At different time intervals, a sample volume of 1.5 mL was transferred and centrifuged at 25,000 g for 10 min. A quantity of 1.0 mL of the supernatant was taken for UV-vis analysis. 1.0 mL of fresh PBS buffer was added to the remaining 0.5 mL sample. 1.5 mL of the suspension was agitated vigorously by vortexing and replaced in the flasks. The cumulative percentage release profiles were obtained by taking the ratio of the amount of CHB released to the total drug content in the same volume of sample.

2.10. Cytotoxicity

To evaluate cytotoxicity, breast cancer cells (MCF-7) and fibroblast cell line (NIH3T3) were obtained from exponentially growing 90% - 95% confluent cultures and seeded at 5000 cells/well in 96-well plates. The cells were kept in 100 µL fresh DMEM media (supplemented by 10% (v/v) FBS, penicillin (50 IU/mL) and streptomycin (50 mg/mL) for 24 h to allow cell adhesion and environmental adaptation. Subsequently, the cells were treated with additional 10 µL PBS containing different concentrations of CHB-NP I and CHB-NP II and in solution for 72 hours. The cell viability was evaluated using the yellow tetrazolium dye (3-(4,5-dimethylthia-zolyl-2) -2,5-diphenyltetrazolium bromide) (MTT) solution. The plates were read at 595 nm using Spectra Max Plate Reader. The percentage of cell viability was calculated with respect to control cells that were incubated without the drug and the nanoparticles as described in previous studies [29] [33] [35]. All experiments were performed in triplicate.

2.11. Statistics

All numerical data are presented as mean ± standard error of the mean (SEM) from at least three independent experiments. Statistical analysis was conducted using the Prism 5.03 software (GraphPad Software, USA). Statistical differences in multiple groups were determined by one-way ANOVA followed by Tukey's test. $P < 0.05$ was considered statistically significant.

3. Results and Discussion

3.1. Method Optimization

Several parameters were systematically investigated to enhance the encapsulation efficiency of CHB in PLGA nanoparticles. Briefly, speed of stirring were modulated to achieve a suitable size for administration; then other properties, such as the particle size distribution, surface charge, crystallinity, and morphology were characterized for both methods of production of CHB-NP I and CHB-NP II.

3.1.1. Influence of Speed Stirring

It is recognized that the degree of agitation influences the stability of the emulsion. Suitable agitation provides the required energy to the system to break up the droplets of the dispersed phase [36]. According to the results shown in **Figure 1**, the smaller hydrodynamic diameter distributions and Poly dispersivity Index (PdI) were achieved in high speed stirring (17,000 rpm) shown for CHB-NP I since CHB-NP II have similar profile.

All of these results are similar to those obtained by Mao *et al*. that prepared FITC-dextran loaded PLGA microspheres [36] [36] when evaluating the parameters for irinote can nanoparticle.

3.1.2. Influence of Drug Concentration and Entrapment Efficiency (%EE)

CHB-NP I and CHB-NP II were evaluated by its capacity of carrying drug. The nanoparticles were assessed using fixed amounts of polymer and surfactant and variable quantities of CHB. According to the results shown in **Table 1**, maximum incorporation efficiencies were achieved for CHB-NP I and CHB-NP II corresponding to a theoretical concentration of 10 mg/mL. For concentrations above 10 mg/mL CHB occurred the precipitation of both CHB and PLGA in the form of crystals, indicating that the maximum loading capacity of the carrier was reached, and this effect is illustrated in **Figure 2** for CHB-NP I.

The nanoparticles produced by double emulsion method (CHB-NP II) and nanoparticles prepared with single emulsion method (CHB-NP I) had similar %EE, CHB-NPI (93.6% ± 2.9%) and CHB-NP II (92.6% ± 2.5%)

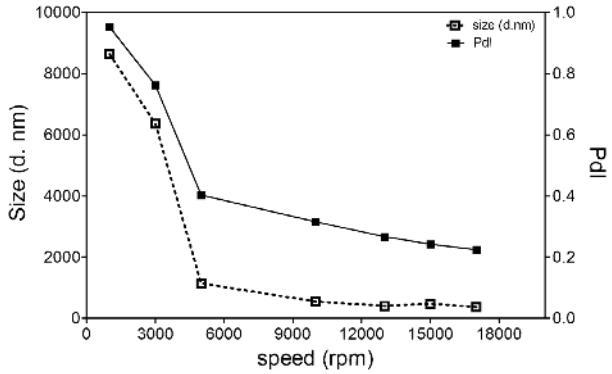

Figure 1. Effect of the speed stirrer on the size (⧟) and polydispersity index (■) of CHB-NP I. Data are shown as mean ± S. E. M. obtained from three formulations.

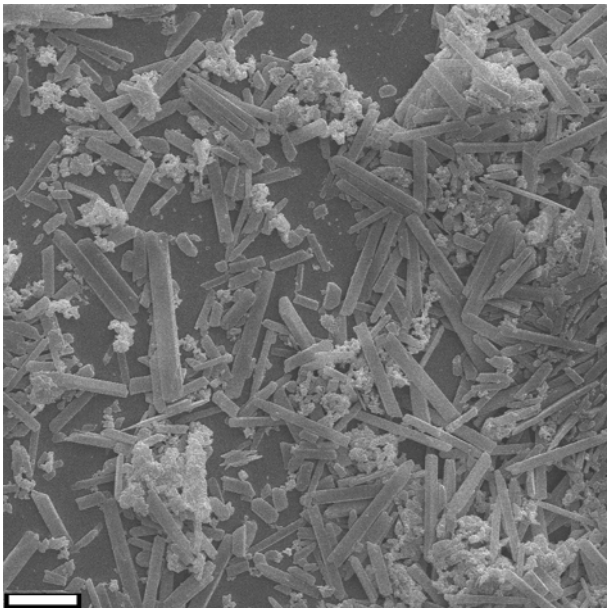

Figure 2. Scanning Electronic Micrograph of CHB-NP I (30 mg), bar 10 μm (magnification 1,000 Å~).

Table 1. Maximum concentration of CHB loading in nanoparticle (mg) and entrapment efficiency (%EE) for CHB-NP I and CHB NP II.

Nanoparticles	%EE
CHB-NP I (10 mg)	93.6 ± 2.9
CHB-NP I (20 mg)	75.6 ± 3.4
CHB-NP I (30 mg)	49.3 ± 4.2
CHB-NP II (10 mg)	92.6 ± 2.5
CHB-NP II (20 mg)	73.8 ± 3.7
CHB-NP II (30 mg)	68.3 ± 3.6

(**Table 1**). The high encapsulation efficiency was observed by other authors using the same drug delivery system to hydrophobic drugs [38]. Most like, this behavior is due to the encapsulation process when the drug is in the organic medium.

3.1.3. Influence of Surfactant Concentration in Size Distribution

Polyvinyl alcohol (PVA) concentrations in the external water phase are known to be a key factor influencing the particle size of nanoparticles. The sizes and PdI of nanoparticles produced at 0.1%, 0.5%, 1.0%, 1.5%, 2.0%, 2.5%, 4.0% and 5.0% PVA are showed in **Figure 3** for CHB-NP I.

Increasing PVA concentration from 0.1 to 5.0% caused approximately 42% particle size decrease. The smaller size particles were obtained when increase PVA concentration from 0.1% to 2.0%, causing reduction in particle size approximately 62%, producing particles having a size of 317 nm. It is well known that the presence of PVA in the external phase stabilizes emulsion droplets against coalescence. The stabilization effect is dominant athigher PVA concentrations and leads to the decrease in the size of nanoparticles [27]. Based on our experimental data, 2.0% PVA seems to be sufficient to prepare both CHB-NP I and CHB-NP II.

3.2. Scanning Electron Microscopy (SM)

Scanning electron microscopy (SM) was used to investigate the morphology of NPs. The SM images of CHB-NP I and CHB-NP II showed NPs with regular spherical shapes (**Figure 4(A)** CHB-NP I) and that their surface morphology was smooth and without evident aggregation. The size distribution of all nanoparticles was

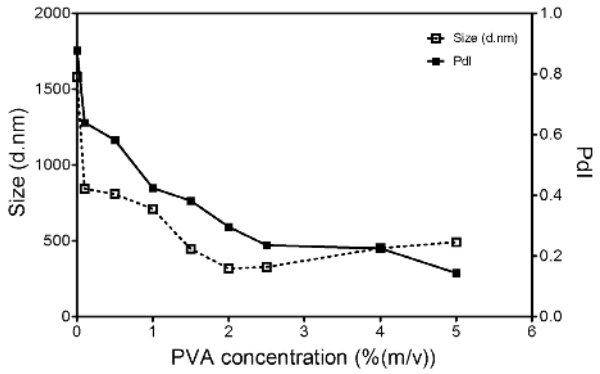

Figure 3. The (□) sizes and (■) polydispersity index of CHB-NP I at different concentrations of PVA.

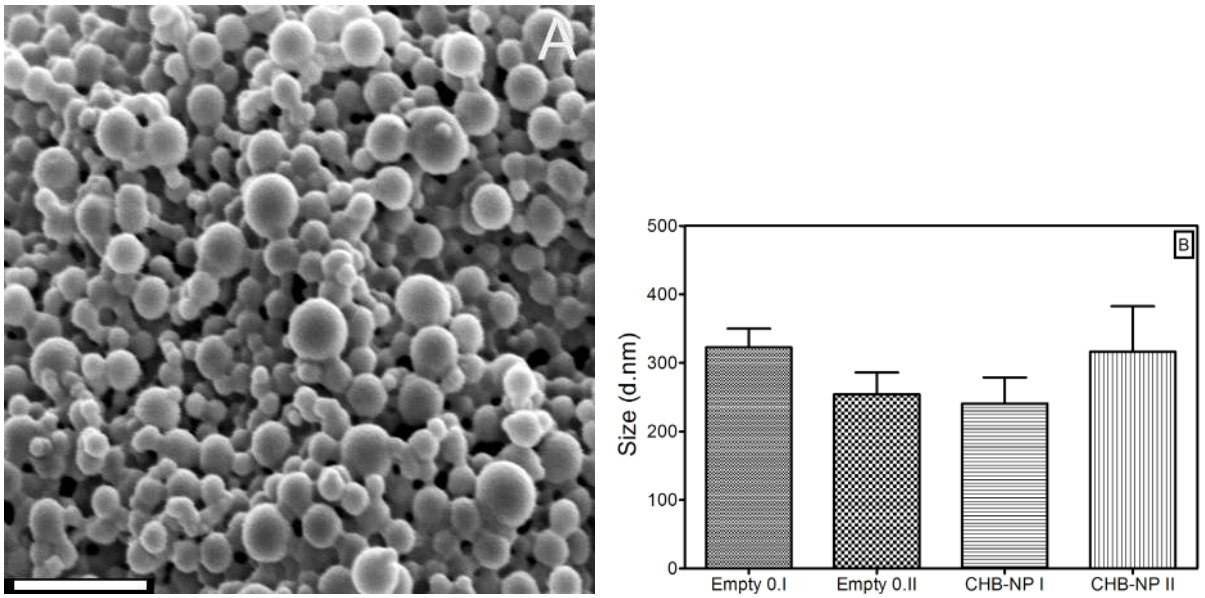

Figure 4. (A) Scanning Electron Microscopy (SM) pictures of CHB-NP I at magnification 10,000 Å~ (scale = 10 μm); (B) Particle diameter measured from the SM image using ImageJ® software.

unimodal with sizes in the range of 240 - 320 nm as confirmed by the morphometric analysis using ImageJ® software (**Figure 4(B)**). Similar morphological results were observed for empty nanoparticles.

3.3. Particle Size and Zeta Potential

Particle sizes and zeta potentials of CHB-NP I and CHB-NP II and empty-NP were determined by employing DLS (n = 3). Nanoparticles size was 238 - 334 nm in diameter with PdI of 0.12 - 0.26 indicating a narrow size distribution (**Table 2**). Similar values were observed using ImageJ® software in SM pictures (**Figure 4(B)**), where particles showed diameters in the range of 240 - 320 nm. As all the NPs were smaller than 500 nm, its parenteral use by intravenous injection is acceptable. No droplets should be larger than 5.0 μm to avoid possible embolism in the lung capillaries [39] [40].

The results of the determination of zeta potential for PLGA nanoparticles without (empty-NP) and with CHB (CHB-NP I and CHB-NP II) ranged between −16.7 and −26.0 mV and are shown in **Table 2**.

Zeta potential is an important physicochemical parameter that influences the stability of the suspension. Extremely positive or negative zeta potential values cause larger repulsive forces, whereas repulsion between particles with similar electric charge prevents aggregation of the particles and thus ensures easy redispersion [41].

The presence of CHB in PLGA nanoparticles decreased the negative zeta potential value; probably, there was a masking effect of the superficial carboxylic groups by the drug adsorbed on nanoparticles surface. The results shown in **Table 2**, confirm the low tendencyof aggregation seen in SM analysis shown in **Figure 4(A)**.

3.4. Infrared Spectrum

FTIR was used to evaluate the chemical structure of CHB-NP I and CHB-NP IIentrapped in PLGA nanoparticles (**Figure 5**). The characteristic peak of PLGA at 1749 cm^{-1} is due to the ester group. During preparation of CHB-NP I, the characteristic peak of PLGA was not altered. The hydroxyl group of PVA was confirmed at 3500 - 3100 cm^{-1}. Furthermore, the CHB characteristic peak of the C-Cl stretching vibrations gives generally strong bands in the region 710 - 505 cm^{-1}. NH group shows its stretching absorption in the region 3500 - 3220 cm^{-1}. The ring carbon-carbon stretching vibrations occur in the region 1625 - 1430 cm^{-1}. The ring C-N stretching vibrations occur in the region 1615 - 1575 cm^{-1} and 1520 - 1465 cm^{-1} [42] [43]. These results suggest that the CHB was successfully entrapped in both CHB-NP I and CHB-NP II (not shown).

3.5. Differential Scanning Calorimetry (DSC)

DSC is a thermal analytical technique, which provides information regarding the physical properties like crystalline or amorphous nature of the samples. This aspect could influence the *in vitro* and *in vivo* release of the drug from the systems. **Figure 6** shows the DSC thermograms corresponding to the following samples: PLGA; empty-NP; CHB-NP I. The PLGA was used as control and thermogram displays an endotherm at 41.2˚C, corresponding to the glass transition temperature (T_g). Empty nanoparticles exhibited endotherms corresponding close to the T_g of PLGA (43.7˚C) due to changes in cristalinity of polymer. For CHB-NP I and CHB-NP II, it observed was a single endothermic peak at 58.8˚C, which suggests the occurrence of an interaction between the polymer (PLGA) and CHB. This interaction is related to covalent bonds between the carboxyl group of polymer and CHB.

As shown in **Figure 6**, NP empty and CHB-NP I have a sharp T_m (melting temperature) that corresponds to their crystal behavior. PLGA shows a T_g (glass to rubber transition temperature) and no T_m that means it isamorphous. Preparation of the NPs has increased the PLGA T_g to higher temperatures; it is because of the crys-

Table 2. Determination of size and zeta potential for CHB-NP I and CHB-NP II.

Nanoparticles	Size (nm)	PdI	Zeta potential (mV)
Empty-NP I	288.90 ± 1.80	0.131 ± 0.028	−26.00 ± 0.45
Empty-NP II	238.40 ± 2.40	0.118 ± 0.025	−23.50 ± 0.35
CHB-NP I	250.30 ± 1.40	0.155 ± 0.031	−17.30 ± 0.2
CHB-NP II	334.40 ± 9.80	0.263 ± 0.026	−16.70 ± 1.07

tallization process during the preparation.

3.6. Release Profile and Spectroscopic Characterization

The CHB release from PLGA nanoparticles was studied in 10 mM PBS (pH 7.4) at 37˚C, which provides a basic idea of the drug release in physiological systems.

The *in vitro* release of CHB-NP I and CHB-NP II were presented as the cumulative percentage releases in **Figure 7**. Drug release from PLGA nanoparticles usually occurs in a two-phase association manner, with an initial burst phase followed by a diffusion-controlled slower drug release phase. In our studies, an initial burst phase corresponding to about 84% to CHB-NP I and 76% to CHB-NP II was observed within 24 hours due to diffusion release of CHB distributed at the surface of the NPs as have been reported by several authors for PLGA nanoparticles [44]. A sustained CHB release to a total of about 92% was found for the nanoparticles over the entire period of study, as depicted in the graph shown in **Figure 7(A)**. Similar results were obtained by Mi and coworkers [45] develop chitin/PLGA 50/50 blend microsphere, were CHB was loaded and show that the release of CHB from a hydrophilic chitin matrix is very quick due to the hydration of chitin matrix and the bulk hydrolysis of dispersed PLGA domain. This similar behavior can be explained by the fact that in general, chlorambucil will be homogeneously dispersed in both chitin and PLGA phase of the blend microsphere [45].

The results indicate the decrease the efficiency of the drug delivery system if applied intravenously (the drug could be released before the nanoparticles reach the target site). These great characteristics turn CHB-NP system

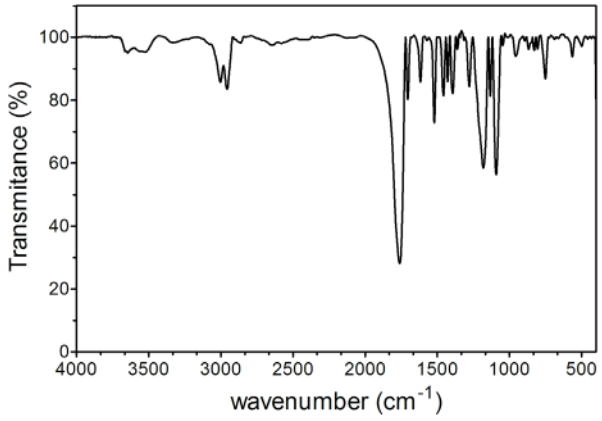

Figure 5. Infrared spectra of dried CHB-NP I. Transmission spectra were recorded using at least 32 scans with 4.0 cm^{-1} resolution, in the spectral range 4000 - 400 cm^{-1}.

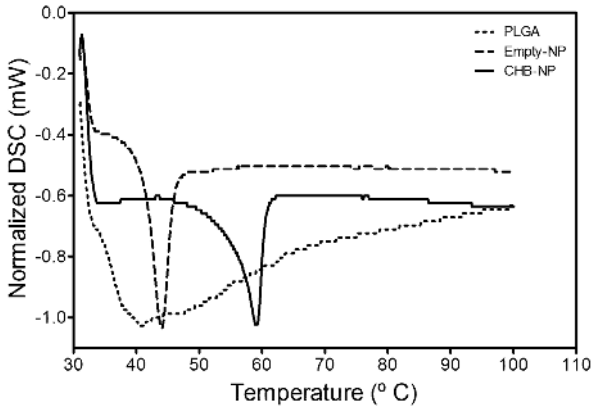

Figure 6. DSC thermograms of (- - -) empty PLGA; (—) CHB-NP I. (---) Pure PLGA was used as a control. The sample (approximately 3.0 mg) was heated twice from 35˚C to 600˚C at 5˚C/min in a nitrogen atmosphere (flow rate 20 mL/min).

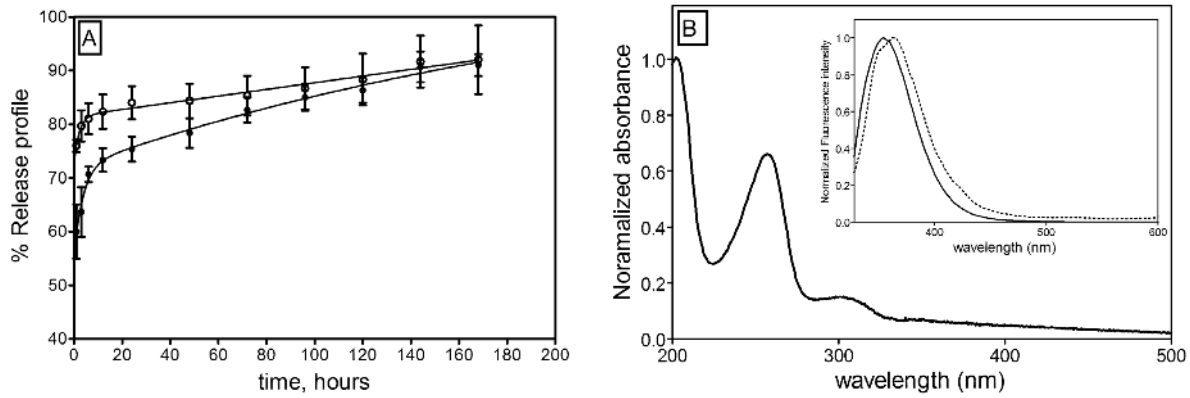

Figure 7. (A) Cumulative release profiles of (□) CHB-NP I and (■) CHB-NP II in phosphate buffer at 37˚C and pH 7.4 after 150 hours. Data are shown as a percentage of the total CHB encapsulated; (B) UV-vis absorption and fluorescence emission spectrum of CHB (contiunuous line) and CHB-NP (dash line).

more suitable for local application (such as intratumoral injection) [13]. The hydrophobic interaction involving the drug and the hydrophobic core of the carriers is a main reason leading to a controlled release rate for the carriers [46].

Also the spectrum profile of the entrapment of CHB in PLGA nanoparticles was done by using UV-vis absorption and fluorescence emission spectrum. The characteristic bands of CHB were observed at 206, 254 and 306 nm, respectively displayed in **Figure 7(B)**. The steady-state emission spectral properties of CHB in mixture methanol/water (1:1), and in the aqueous medium with nanoparticles, were shown to have excitation wavelengths for CHB at 260 and 310 nm, respectively. The emission spectra of CHB-NP I and free CHB were evaluated using fluorescence emission spectroscopy (**Figure 7(B)**). The maximum emission spectrum of CHB occurs around 354 nm, and in CHB-NP I around 364 nm (bathochromic shift = 10 nm). The bathochromic shift can be attributed to difference in index of refraction of the media also indicating the efficient encapsulation of the drug in the polymer matrix. Since the polymer itself does not emitfluorescence.

3.7. Cytotoxicity Assay

We report the effects of CHB and CHB-NP I and CHB-NP II on the growth of the fibroblast cell line (NIH3T3) and human breast cancer cell MCF-7. It has been well established that the MCF-7 cell line is a powerful tool for the study of breast cancer resistance to chemotherapy, because it appears to mirror the heterogeneity of tumor cells *in vivo* [47]. The cytotoxicity of the CHB was evaluated using the MTT assay, an established *in vitro* cytotoxicity assay measuring the reduction of 3-[4,5-dimethylthiazol-2-yl]-2,5-diphenyltetrazolium bromide by intracellular reductases, the content [28] [29] [33]. To evaluate the possible cytotoxic effect of the CHB-NP I and CHB-NP II on the survival rates of MCF-7 and NIH3T3 the cells were incubated with the nanoparticles for 72 h, and assayed for cell viability by the MTT test (**Figure 8(A)** and **Figure 8(B)**). The cytotoxicity of both CHB-NPs and free CHB were evaluated in NIH3T3 and MCF-7 displayed a significant dose-dependent profile. In literature it had been described different effects of cytotoxic behaviors depending on the type of drug, concentration, drug-delivery system and cell line type. Fonseca and coworkers [48] evaluated the *in vitro* anti-tumoral activity of paclitaxel (Taxol) incorporated in the PLGA nanoparticles in human small cell lung cancer cell line (NCI-H69) and showed that incorporation of paclitaxel in the nanoparticles strongly enhances its anti-tumoral efficacy as compared to the free drug [48]. Danhier [25] developed paclitaxel-loaded, PEGylated, PLGA-based nanoparticle and as indicated by cell viability studies, paclitaxel-loaded nanoparticles are more cytotoxic toward human cervix carcinoma cells (HeLa), compared with free Taxol. Another profile was described by Averineni [49] evaluating antitumor activity of PLGA 50:50 nanoparticles entrapped with paclitaxel in BT-549 cells tested in concentrations 10 μg/mL with significant differences in the cytotoxicity effect of paclitaxel loaded nanoparticles and free drug. Mukerjee [50] evaluated the antitumoral activity of curcumin-loaded PLGA nanospheres on prostate cancer cell lines, LNCaP, PC3, DU145, and PWR1E. The cell viability assay showed that the IC50 of curcumin-loaded PLGA nanoparticles and free curcumin was similar for 31 μM and 37 μM respectively. In recent study Pirooznia [51] evaluated cell cytotoxicity ofα1AT-loaded nanoparticles using

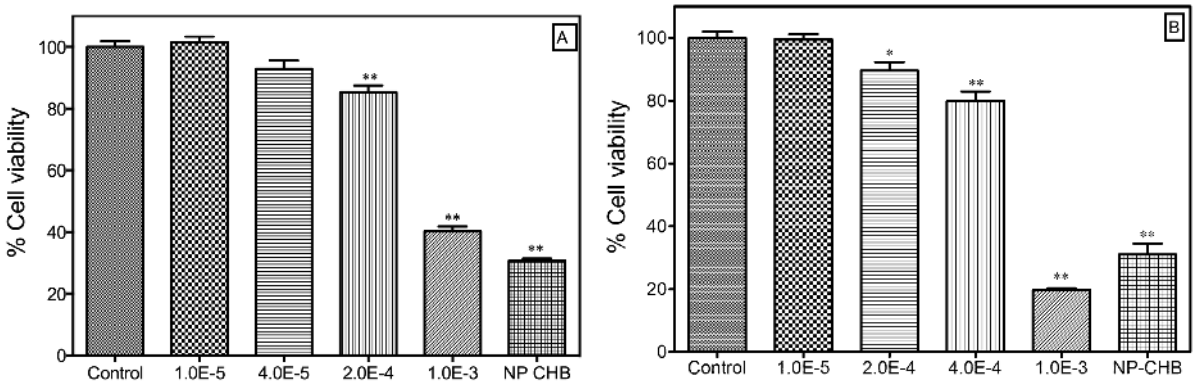

Figure 8. Cytotoxicity of free CHB and CHB-NP against (A) NIH3T3 cells and (B) MCF-7 cells after 72 hours of treatment. Cell viability was assessed by MTT assay and compared to the control (100% cell viability). Data are expressed as mean ± SEM. $^{**}P < 0.01$ was considered to be statistically significant compared to the control group using Turkey's multiple comparision test.

Cor L105 lung epithelial-like cells. The results show that the viability of cells treated with free and loaded nanoparticles remains unchanged. Ribeiro-Costa [52] evaluated usnic acid encapsulated into PLGA-microspheres, the cytotoxic effect of free and encapsulated usnic acid was evaluated on HEp-2 cells and no significant difference between the cytotoxicity of free and encapsulated usnic acid was observed, presenting the same IC50 magnitude order.

In **Figure 8(A)** it is displayed the cell viability assay for free CHB and CHB-NP against NIH3T3 cells. After 72 h of incubation the cell viability assay showed a 59.7% ($P < 0.0001$) and 69.3% ($P < 0.0001$) of reduction on cell survival respectively. Turkey's multiple comparisons test show that CHB free 1.0×10^{-3} M and NP CHB are significant different of control and among than in NH3T3 cell line. The free CHB showed a reduction of 81.3% on cell viability at 1.0×10^{-3} M ($P < 0.05$), while the CHB-NP (10^{-3} M) display 68.9% ($P < 0.001$) in MCF-7 cells (**Figure 8(B)**). Tukey's multiple comparisons test show that CHB free 1.0×10^{-3} M and NP CHB are significant different of control but not different in MCF-7 cell line. In the case of empty nanoparticles, the samples did not show cytotoxicity towards the MCF-7 and NIH3T3cell lines during test period (cell viability exceeded 90%).

4. Conclusion

Our analyses characterizes the formulation of CHB-PLGA nanoparticles applying double emulsion method and solvent evaporation process to improve the physic chemical characteristics of the drug delivery system. The size and entrapment efficiency of the nanoparticles can be adjusted by modifying various parameters, such as, drug/polymer ratio, surfactant concentration and speed of homogenization. The smaller size and high erentrapment efficiency was obtained directing the lower amount of drug, intermediate concentration surfactant and higher agitation speed. The UV-vis spectroscopic as say indicated the potential use of PLGA nanoparticles for sustained release of lipophilic drugs such as CHB as demonstrated in the release profile. A cytotoxicity study revealed that empty NP had no cytotoxicity, while both CHB-NP I and CHB-NP II showed similar antitumor activities as free chlorambucil after 72 h. In conclusion, the developed PLGA-CHB nanoparticles could be considered as an effective strategy for application of this drug in cancer therapy using nanotechnology.

Declaration of Interest

The authors report no conflict of interest. The authors alone are responsible for the content and writing of this article.

Acknowledgements

The authors are grateful to CNPq, CAPES, FAPDF, FINATEC and DPP for financial support of this research.

References

[1] Zhang, H., Ye, Z.W. and Lou, Y.J. (2004) Metabolism of Chlorambucil by Rat Liver Microsomal Glutathione S-

Transferase. *Chemico-Biological Interactions*, **149**, 61-67. http://dx.doi.org/10.1016/j.cbi.2003.07.002

[2] Schmidt, M. (2014) Chemotherapy in Early Breast Cancer: When, How and Which One? *Breast Care* (*Basel*), **9**, 154-160. http://dx.doi.org/10.1159/000363755

[3] Cummings, S.R., Tice, J.A., Bauer, S., Browner, W.S., Cuzick, J., Ziv, E., Vogel, V., Shepherd, J., Vachon, C., Smith-Bindman, R. and Kerlikowske, K. (2009) Prevention of Breast Cancer in Postmenopausal Women: Approaches to Estimating and Reducing Risk. *Journal of the National Cancer Institute*, **101**, 384-398. http://dx.doi.org/10.1093/jnci/djp018

[4] Zhang, W.J., Feng, M.L., Zheng, G.P., Chen, Y., Wang, X.D., Pen, B., Yin, J., Yu, Y.H. and He, Z.M. (2012) Chemoresistance to 5-Fluorouracil Induces Epithelial-Mesenchymal Transition via Up-Regulation of Snail in MCF7 Human Breast Cancer Cells. *Biochemical and Biophysical Research Communications*, **417**, 679-685. http://dx.doi.org/10.1016/j.bbrc.2011.11.142

[5] Bergh, J., Jonsson, P.E., Glimelius, B., Nygren, P. and Care, S.B.-G.S.C.O.T.A.I.H. (2001) A Systematic Overview of Chemotherapy Effects in Breast Cancer. *Acta Oncologica*, **40**, 253-281. http://dx.doi.org/10.1080/02841860151116349

[6] Anderson, W.F., Rosenberg, P.S., Prat, A., Perou, C.M. and Sherman, M.E. (2014) How Many Etiological Subtypes of Breast Cancer: Two, Three, Four, or More? *Journal of the National Cancer Institute*, **106**, 1-11.

[7] Pettersson, A., Graff, R.E., Ursin, G., Santos Silva, I.D., McCormack, V., Baglietto, L., Vachon, C., Bakker, M.F., Giles, G.G., Chia, K.S., Czene, K., Eriksson, L., Hall, P., Hartman, M., Warren, R.M., Hislop, G., Chiarelli, A.M., Hopper, J.L., Krishnan, K., Li, J., Li, Q., Pagano, I., Rosner, B.A., Wong, C.S., Scott, C., Stone, J., Maskarinec, G., Boyd, N.F., van Gils, C.H. and Tamimi, R.M. (2014) Mammographic Density Phenotypes and Risk of Breast Cancer: A Meta-Analysis. *Journal of the National Cancer Institute*, **106**, 1-11.

[8] Bielawski, K., Bielawska, A., Muszynska, A., Poplawska, B. and Czarnomysy, R. (2011) Cytotoxic Activity of G3 PAMAM-NH2 Dendrimer-Chlorambucil Conjugate in Human Breast Cancer Cells. *Environmental Toxicology and Pharmacology*, **32**, 364-372. http://dx.doi.org/10.1016/j.etap.2011.08.002

[9] Benitah, N., de Lorimier, L.-P., Gaspar, M. and Kitchell, B.E. (2003) Chlorambucil-Induced Myoclonus in a Cat with Lymphoma. *Journal of the American Animal Hospital Association*, **39**, 283-287. http://dx.doi.org/10.5326/0390283

[10] Hehn, S.T., Dorr, R.T. and Miller, T.P. (2003) Mood Alterations in Patients Treated with Chlorambucil. *Clinical lymphoma*, **4**, 179-182. http://dx.doi.org/10.3816/CLM.2003.n.028

[11] Reux, B., Weber, V., Galmier, M.J., Borel, M., Madesclaire, M., Madelmont, J.C., Debiton, E. and Coudert, P. (2008) Synthesis and Cytotoxic Properties of New Fluorodeoxyglucose-Coupled Chlorambucil Derivatives. *Bioorganic & Medicinal Chemistry*, **16**, 5004-5020. http://dx.doi.org/10.1016/j.bmc.2008.03.038

[12] Ganta, S., Paxton, J.W., Baguley, B.C. and Garg, S. (2008) Pharmacokinetics and Pharmacodynamics of Chlorambucil Delivered in Parenteral Emulsion. *International Journal of Pharmaceutics*, **360**, 115-121. http://dx.doi.org/10.1016/j.ijpharm.2008.04.027

[13] Yordanov, G.G., Bedzhova, Z.A. and Dushkin, C.D. (2010) Preparation and Physicochemical Characterization of Novel Chlorambucil-Loaded Nanoparticles of Poly(Butylcyanoacrylate). *Colloid and Polymer Science*, **288**, 893-899. http://dx.doi.org/10.1007/s00396-010-2219-5

[14] Descoteaux, C., Leblanc, V., Brasseur, K., Gupta, A., Asselin, E. and Berube, G. (2010) Synthesis of $_{D}$- and $_{L}$-Tyrosine-Chlorambucil Analogs Active against Breast Cancer Cell Lines. *Bioorganic & Medicinal Chemistry Letters*, **20**, 7388-7392. http://dx.doi.org/10.1016/j.bmcl.2010.10.039

[15] Omoomi, F.D. (2013) Molecular Chlorambucil-Methionine Conjugate: Novel Anti-Cancer Agent against Breast MCF-7 Cell Model. *Journal of Cancer Science & Therapy*, **5**, 75-84.

[16] Millard, M., Gallagher, J.D., Olenyuk, B.Z. and Neamati, N. (2013) A Selective Mitochondrial-Targeted Chlorambucil with Remarkable Cytotoxicity in Breast and Pancreatic Cancers. *Journal of Medicinal Chemistry*, **56**, 9170-9179. http://dx.doi.org/10.1021/jm4012438

[17] Gomes, A.J., Barbougli, P.A., Espreafico, E.M. and Tfouni, E. (2008) Trans-$[Ru(NO)(NH_3)_4(py)](BF_4)_3 \cdot H_2O$ Encapsulated in PLGA Microparticles for Delivery of Nitric Oxide to B16-F10 Cells: Cytotoxicity and Phototoxicity. *Journal of Inorganic Biochemistry*, **102**, 757-766. http://dx.doi.org/10.1016/j.jinorgbio.2007.11.012

[18] Gomes, A.J., Espreafico, E.M. and Tfouni, E. (2013) Trans-[Ru(NO)Cl(Cyclam)]$(PF_6)_2$ and [Ru(NO)(Hedta)] Incorporated in PLGA Nanoparticles for the Delivery of Nitric Oxide to B16-F10 Cells: Cytotoxicity and Phototoxicity. *Molecular Pharmaceutics*, **10**, 3544-3554.

[19] Birnbaum, D., Kosmala, J. and Brannon-Peppas, L. (2000) Optimization of Preparation Techniques for Poly(Lactic Acid-Co-Glycolic Acid) Nanoparticles. *Journal of Nanoparticle Research*, **2**, 173-181. http://dx.doi.org/10.1023/A:1010038908767

[20] Kranz, H. and Bodmeier, R. (2007) A Novel *in Situ* Forming Drug Delivery System for Controlled Parenteral Drug Delivery. *International Journal of Pharmaceutics*, **332**, 107-114. http://dx.doi.org/10.1016/j.ijpharm.2006.09.033

[21] Vandervoort, J. and Ludwig, A. (2002) Biocompatible Stabilizers in the Preparation of PLGA Nanoparticles: A Factorial Design Study. *International Journal of Pharmaceutics*, **238**, 77-92. http://dx.doi.org/10.1016/S0378-5173(02)00058-3

[22] Wischke, C. and Schwendeman, S.P. (2008) Principles of Encapsulating Hydrophobic Drugs in PLA/PLGA Microparticles. *International Journal of Pharmaceutics*, **364**, 298-327. http://dx.doi.org/10.1016/j.ijpharm.2008.04.042

[23] Locatelli, E. and Comes Franchini, M. (2012) Biodegradable PLGA-b-PEG Polymeric Nanoparticles: Synthesis, Properties, and Nanomedical Applications as Drug Delivery System. *Journal of Nanoparticle Research*, **14**, 1-17. http://dx.doi.org/10.1007/s11051-012-1316-4

[24] Manchanda, R., Fernandez-Fernandez, A., Nagesetti, A. and McGoron, A.J. (2010) Preparation and Characterization of a Polymeric (PLGA) Nanoparticulate Drug Delivery System with Simultaneous Incorporation of Chemotherapeutic and Thermo-Optical Agents. *Colloids and Surfaces B*: *Biointerfaces*, **75**, 260-267. http://dx.doi.org/10.1016/j.colsurfb.2009.08.043

[25] Danhier, F., Ansorena, E., Silva, J.M., Coco, R., Le Breton, A. and Preat, V. (2012) PLGA-Based Nanoparticles: An Overview of Biomedical Applications. *Journal of Controlled Release*, **161**, 505-522. http://dx.doi.org/10.1016/j.jconrel.2012.01.043

[26] Makadia, H.K. and Siegel, S.J. (2011) Poly Lactic-co-Glycolic Acid (PLGA) as Biodegradable Controlled Drug Delivery Carrier. *Polymers* (*Basel*), **3**, 1377-1397. http://dx.doi.org/10.3390/polym3031377

[27] Mao, S., Xu, J., Cai, C., Germershaus, O., Schaper, A. and Kissel, T. (2007) Effect of WOW Process Parameters on Morphology and Burst Release of FITC-Dextran Loaded PLGA Microspheres. *International Journal of Pharmaceutics*, **334**, 137-148. http://dx.doi.org/10.1016/j.ijpharm.2006.10.036

[28] Gomes, A.J., Assuncao, R.M.N., Rodrigues, G., Espreafico, E.M. and Machado, A.E.D. (2007) Preparation and Characterization of Poly(D,L-lactic-*co*-glycolic Acid) Nanoparticles Containing 3-(Benzoxazol-2-yl)-7-(*N*,*N*-diethyl amino)chromen-2-one. *Journal of Applied Polymer Science*, **105**, 964-972. http://dx.doi.org/10.1002/app.26204

[29] Gomes, A.J., Faustino, A.S., Lunardi, C.N., Lunardi, L.O. and Machado, A.E.H. (2007) Evaluation of Nanoparticles Loaded with Benzopsoralen in Rat Peritoneal Exudate Cells. *International Journal of Pharmaceutics*, **332**, 153-160. http://dx.doi.org/10.1016/j.ijpharm.2006.09.035

[30] Gomes, A.J., Lunardi, L.O., Marchetti, J.M., Lunardi, C.N. and Tedesco, A.C. (2005) Photobiological and Ultrastructural Studies of Nanoparticles of Poly(lactic-*co*-glycolic Acid)-Containing Bacteriochlorophyll-*a* as a Photosensitizer Useful for PDT Treatment. *Drug Delivery*, **12**, 159-164. http://dx.doi.org/10.1080/10717540590931846

[31] Gomes, A.J., Lunardi, C.N., Lunardi, L.O., Pitol, D.L. and Machado, A.E.H. (2008) Identification of Psoralen Loaded PLGA Microspheres in Rat Skin by Light Microscopy. *Micron*, **39**, 40-44. http://dx.doi.org/10.1016/j.micron.2007.06.015

[32] Gomes, A.J., Faustino, A.S., Machado, A.E.H., Zaniquelli, M.E.D., Rigoletto, T.D., Lunardi, C.N. and Lunardi, L.O. (2006) Characterization of PLGA Microparticles as a Drug Carrier for 3-Ethoxycarbonyl-2H-benzofuro[3,2-f]-1-benzopyran-2-one. Ultrastructural Study of Cellular Uptake and Intracellular Distribution. *Drug Delivery*, **13**, 447-454. http://dx.doi.org/10.1080/10717540600640369

[33] Tfouni, E., Truzzi, D.R., Tavares, A., Gomes, A.J., Figueiredo, L.E. and Franco, D.W. (2012) Biological Activity of Ruthenium Nitrosyl Complexes. *Nitric Oxide-Biology and Chemistry*, **26**, 38-53. http://dx.doi.org/10.1016/j.niox.2011.11.005

[34] Tfouni, E., Doro, F.G., Gomes, A.J., da Silva, R.S., Metzker, G., Benini, P.G.Z. and Franco, D.W. (2010) Immobilized Ruthenium Complexes and Aspects of Their Reactivity. *Coordination Chemistry Reviews*, **254**, 355-371. http://dx.doi.org/10.1016/j.ccr.2009.10.011

[35] Gomes, A.J., Lunardi, L.O., Caetano, F.H., Machado, A.E.H., Oliveira-Campos, A.M.F., Bendhack, L.M. and Lunardi, C.N. (2011) Biodegradable Nanoparticles Containing Benzopsoralens: An Attractive Strategy for Modifying Vascular Function in Pathological Skin Disorders. *Journal of Applied Polymer Science*, **121**, 1348-1354. http://dx.doi.org/10.1002/app.33427

[36] Mo, L., Hou, L., Guo, D., Xiao, X., Mao, P. and Yang, X. (2012) Preparation and Characterization of Teniposide PLGA Nanoparticles and Their Uptake in Human Glioblastoma U87MG Cells. *International Journal of Pharmaceutics*, **436**, 815-824. http://dx.doi.org/10.1016/j.ijpharm.2012.07.050

[37] Wang, Y.C., Xu, G.L., Jia, W.D., Han, S.J., Ren, W.H., Wang, W., Liu, W.B., Zhang, C.H. and Chen, H. (2012) Estrogen Suppresses Metastasis in Rat Hepatocellular Carcinoma through Decreasing Interleukin-6 and Hepatocyte Growth Factor Expression. *Inflammation*, **35**, 143-149. http://dx.doi.org/10.1007/s10753-011-9299-3

[38] Jyothi, N.V.N., Prasanna, P.M., Sakarkar, S.N., Prabha, K.S., Ramaiah, P.S. and Srawan, G.Y. (2010) Microencapsulation Techniques, Factors Influencing Encapsulation Efficiency. *Journal of Microencapsulation*, **27**, 187-197. http://dx.doi.org/10.3109/02652040903131301

[39] Song, H., Nie, S., Yang, X., Li, N., Xu, H., Zheng, L. and Pan, W. (2010) Characterization and *in Vivo* Evaluation of Novel Lipid-Chlorambucil Nanospheres Prepared Using a Mixture of Emulsifiers for Parenteral Administration. *International Journal of Nanomedicine*, **5**, 933-942. http://dx.doi.org/10.2147/IJN.S14596

[40] de Jesus Gomes, A., Lunardi, C.N., Caetano, F.H., Lunardi, L.O. and da Hora Machado, A.E. (2006) Phagocytosis of PLGA Microparticles in Rat Peritoneal Exudate Cells: A Time-Dependent Study. *Microscopy and Microanalysis*, **12**, 399-405. http://dx.doi.org/10.1017/S1431927606060284

[41] Gupta, H., Aqil, M., Khar, R.K., Ali, A., Bhatnagar, A. and Mittal, G. (2010) Sparfloxacin-Loaded PLGA Nanoparticles for Sustained Ocular Drug Delivery. *Nanomedicine*: *Nanotechnology Biology and Medicine*, **6**, 324-333. http://dx.doi.org/10.1016/j.nano.2009.10.004

[42] Gunasekaran, S., Kumaresan, S., Balaji, R.A., Anand, G. and Seshadri, S. (2008) Vibrational Spectra and Normal Coordinate Analysis on Structure of Chlorambucil and Thioguanine. *Pramana*: *Journal of Physics*, **71**, 1291-1300. http://dx.doi.org/10.1007/s12043-008-0183-0

[43] Yang, J., Lee, C.H., Park, J., Seo, S., Lim, E.K., Song, Y.J., Suh, J.S., Yoon, H.G., Huh, Y.M. and Haam, S. (2007) Antibody Conjugated Magnetic PLGA Nanoparticles for Diagnosis and Treatment of Breast Cancer. *Journal of Materials Chemistry*, **17**, 2695-2699. http://dx.doi.org/10.1039/b702538f

[44] Garcia, X., Escribano, E., Domenech, J., Queralt, J. and Freixes, J. (2011) *In Vitro* Characterization and *in Vivo* Analgesic and Anti-Allodynic Activity of PLGA-Bupivacaine Nanoparticles. *Journal of Nanoparticle Research*, **13**, 2213-2223. http://dx.doi.org/10.1007/s11051-010-9979-1

[45] Mi, F.L., Lin, Y.M., Wu, Y.B., Shyu, S.S. and Tsai, Y.H. (2002) Chitin/PLGA Blend Microspheres as a Biodegradable Drug-Delivery System: Phase-Separation, Degradation and Release Behavior. *Biomaterials*, **23**, 3257-3267. http://dx.doi.org/10.1016/S0142-9612(02)00084-4

[46] Namazi, H. and Jafarirad, S. (2011) *In Vitro* Photo-Controlled Drug Release System Based on Amphiphilic Linear-Dendritic Diblock Copolymers; Self-Assembly Behavior and Application as Nanocarrier. *Journal of Pharmaceutical Sciences*, **14**, 162-180.

[47] Ray, R.S., Rana, B., Swami, B., Venu, V. and Chatterjee, M. (2006) Vanadium Mediated Apoptosis and Cell Cycle Arrest in MCF7 Cell Line. *Chemico-Biological Interactions*, **163**, 239-247. http://dx.doi.org/10.1016/j.cbi.2006.08.006

[48] Fonseca, C., Simoes, S. and Gaspar, R. (2002) Paclitaxel-Loaded PLGA Nanoparticles: Preparation, Physicochemical Characterization and *in Vitro* Anti-Tumoral Activity. *Journal of Controlled Release*, **83**, 273-286. http://dx.doi.org/10.1016/S0168-3659(02)00212-2

[49] Averineni, R.K.S., Shavi, G.V., Gurram, A.K., Deshpande, P.B., Arumugam, K., Maliyakkal, N., Meka, S.R. and Nayahirama, U. (2012) PLGA 50:50 Nanoparticles of Paclitaxel: Development, *in Vitro* Anti-Tumor Activity in BT-549 Cells and *in Vivo* Evaluation. *Bulletin of Materials Science*, **35**, 319-326. http://dx.doi.org/10.1007/s12034-012-0313-7

[50] Mukerjee, A. and Vishwanatha, J.K. (2009) Formulation, Characterization and Evaluation of Curcumin-Loaded PLGA Nanospheres for Cancer Therapy. *Anticancer Research*, **29**, 3867-3875.

[51] Pirooznia, N., Hasannia, S., Lotfi, A.S. and Ghanei, M. (2012) Encapsulation of Alpha-1 Antitrypsin in PLGA Nanoparticles: *In Vitro* Characterization as an Effective Aerosol Formulation in Pulmonary Diseases. *Journal of Nanobiotechnology*, **10**, 1-15.

[52] Ribeiro-Costa, R.M., Alves, A.J., Santos, N.P., Nascimento, S.C., Goncalves, E.C., Silva, N.H., Honda, N.K. and Santos-Magalhaes, N.S. (2004) *In Vitro* and *in Vivo* Properties of Usnic Acid Encapsulated into PLGA-Microspheres. *Journal of Microencapsulation*, **21**, 371-384. http://dx.doi.org/10.1080/02652040410001673919

Scientific Research Publishing (SCIRP) is one of the largest Open Access journal publishers. It is currently publishing more than 200 open access, online, peer-reviewed journals covering a wide range of academic disciplines. SCIRP serves the worldwide academic communities and contributes to the progress and application of science with its publication.

Other selected journals from SCIRP are listed as below. Submit your manuscript to us via either submit@scirp.org or Online Submission Portal.